**A Thesis for the Degree of Master of Science**

# Orobol, an Enzyme-Converted Product of Genistein, Suppresses Obesity by Targeting Casein Kinase 1 epsilon

# Casein Kinase 1 epsilon 활성 저해를 통한 오로볼의 비만 억제 효능

**February, 2016**

**By**

**Hae Ji**

**Department of Agricultural Biotechnology**

**Seoul National University**

## Abstract

Obesity is one of the most important risk factors in the various diseases including type 2 diabetes, cardiovascular diseases, and multiple forms of cancers. Due to side-effects of anti-obesity drugs, natural materials have been studied to be used as alternatives for obesity treatment. There have been many evidences that isoflavones derived from soybean play a beneficial role in obesity. In the present study, the anti-obesity effect of orobol which is one of soy isoflavones has been investigated in adipogenic cocktail (MDI)-induced 3T3-L1 adipocytes and high-fat diet (HFD)-induced male C57BL/6J obese mice model. During MDI-induced adipogenesis in 3T3-L1 pre-adipocytes, orobol 20 μM suppressed lipid accumulation and decreased protein expression levels of peroxisome proliferator-activated receptor-γ (PPARγ), CCAT/ enhancer-binding protein-α (C/EBPα) and fatty acid synthase (FAS). Orobol blocked adipogenesis from early stage to

terminal differentiation by inhibiting Casein Kinase 1 epsilon (CK1ε) and its downstream signaling pathways, eukaryotic translation initiation factor 4E-binding protein 1 (4E-BP1) in 3T3-L1 preadipocytes. Also orobol treatment resulted in reduced lipid accumulation in HFD-fed mice model. In summary, I firstly identified orobol significantly suppressed adipogenesis and this inhibitory effect exerted through CK1ε/4E-BP1 in 3T3-L1 preadipocytes. These findings suggest orobol can be a novel therapeutic agent to treat obesity.

**Keywords: Orobol; 5,7,3′,4′-Tetrahydroxyisoflavone; Obesity; Adipogenesis; CK1ε; 4E-BP1; 3T3-L1 preadipocytes; C57BL/6J mice**

**Student ID: 2014-20720**

# Contents

## Ⅰ. Introduction

Obesity is defined as excessive fat accumulation that is sufficient to adversely affect health [1]. The growing prevalence of obesity and overweight has become a worldwide health problem with significant social costs [2]. During over nutrition, adipose tissue gets bigger through a combination of hypertrophy (increase in cell size) and hyperplasia (increase in cell number) [3]. Therefore, hypertrophy and hyperplasia of adipocytes can be crucial targets for treating obesity.

Adipogenesis is a multi-step process leading to adipocyte development [5, 6]. Adipocytes are critical regulators of whole-body metabolism and are created from precursor cells [4]. Adipocyte differentiation involves a temporally regulated set of gene-expression events including the nuclear receptor peroxisome proliferator activated receptor γ (PPARγ) and CCAAT/enhancer-binding protein (C/EBPα). Adipogenesis consists of early stage of proliferation and terminal

differentiation [7]. The essential phase of adipogenesis inhibition is proliferative step including mitotic clonal expansion (MCE).

Previous studies have shown that eukaryotic translation initiation factor 4E-binding protein 1 (4E-BP1) is a novel regulator of adipogenesis and metabolism in mammals [8-12]. 4E-BP1 plays a critical role in controlling biological processes, such as cell proliferation and protein synthesis [13]. The importance of 4E-BP1 is inhibition of mRNA translation initiation by binding to eukaryotic translation initiation factor 4E (eIF4E) [14]. 4E-BP1 phosphorylation results in eIF4E release, thereby enabling cap-translation initiation [15].

CK1ε is a major regulator of 4E-BP1 phosphorylation that affects adipogenesis activation [21]. Casein kinase 1 (CK1) is the key kinase that regulates circadian rhythm. Circadian rhythms govern a remarkable variety of metabolic and physiological functions [16-18]. CK1 family phosphorylates crucial regulatory proteins including cell

proliferation, differentiation, and circadian rhythms [19]. Among them, CK1ε is especially required for breast cell proliferation [20]. Also, the result of previous study showed that CK1ε was the most effectively inhibited by oriole among whole human kinases.

Anti-obesity drugs have several side-effects, including dry mouth, blood pressure, constipation, headache, and insomnia. For this reason, natural materials have been focused on the alternative strategy for combating obesity [22]. In Asian countries, diet consists highly of soy and soy-based products. The lower frequency of obesity and related metabolic diseases in these countries is associated with soy consumption especially content of isoflavones [23].

Orobol is an isoflavone derived from soybean. Orobol exists in nature or is yielded during the fermentation of soybeans or metabolism in the body [24, 25]. Orobol is structurally similar to genistein which is the most prevalent soy isoflavone. Soy isoflavones, especially genistein

has been well known as an anti-obesity agent [26-28]. Genistein is hydroxylated to form orobol in the body and orobol formation is essential for its cellular activity [29]. Orobol has been reported the inhibitory effect on angiogenesis and endothelial, cancer cell proliferation [25, 30, 31]. However, orobol has not been proved the anti-obesity effect. In this study, I showed anti-obesity effects of orobol *in vitro*, *in vivo* and identified a direct target of orobol in 3T3-L1 preadipocytes. Orobol effectively inhibited adipocyte formation and adipose tissue growth because of the structure which can do cellular function.

## Ⅱ. Materials and methods

### 2.1. Reagents

Orobol was provided from Prof. Byung-Gee Kim's laboratory in Seoul National University. It was produced from bioconversion by tyrosinase in *Bacillus megaterium* [41]. Genistin, genistein, daidzin, daidzein, and equol were purchased from Sigma-Aldrich (St. Louis, MO). 6,7,4'-Trihydroxyisoflavone (6-ODI) was obtained from Chromadex™ (Irvine, CA). 7,3',4'-Trihydroxyisoflavone (3'-ODI) and 7,8,4'-Trihydroxyisoflavone (8-ODI) were purchased from Indofine Chemical (Hillsborough, NJ).

## 2.2. Cell culture and preadipocyte differentiation

3T3-L1 preadipocytes were purchased from American Type Culture Collection (ATCC) (Manassas, VA). Dulbecco's modified eagle medium (DMEM), fetal bovine serum (FBS) and bovine calf serum (BCS) were purchased from GIBCO (Grand Island, NY). Methylisobutylxantine (IBMX), dexamethasone, human insulin were purchased from Sigma-Aldrich (St. Louis, MO). 3T3-L1 preadipoctyes were maintained in DMEM supplemented with 10% BCS, at 5% $CO_2$ and 37 ℃ until 100% confluence. After post-confluent (day 0), cells were incubated in DMEM supplemented with 10% fetal bovine serum (FBS) and adipogenic cocktail (MDI) which is a mixture of 0.5 mM 3-isobutyl-1-methylcanthine (IBMX), 1 μM dexamethasone (DEX) and 5 μg/mL insulin for 2 days in order to induce differentiation. After 2 days, medium was changed to DMEM containing 10% FBS and 5 μg/mL insulin. Two days later, medium were switched to DMEM containing 10% FBS until preadipocytes were fully differentiated.

## 2.3. Cell proliferation assay

3-[4,5-diethylthiazol-2-yl]-2,5-diphenyltetrazolium bromide (MTT) was purchased from USB (Cleveland, OH). Dimethylsulfoxide (DMSO) was purchased from Duksan (Ansan, South Korea). 3T3-L1 preadipocytes were seeded in 24-well plate at a density of 5.0 x $10^4$ cells per well. After confluence, chemicals were treated at the concentration of 5, 10, 20, 40, and 80 μM for 72 hours. Subsequent incubation of the cells with MTT solution (0.5 mg/mL) for 1 hour at 37 ℃ to allow formation of violet crystals (formazan). Crystal form of formazan was dissolved in DMSO and the absorbance was measured at 595 nm with a microplate reader (Beckman-Coulter, CA).

## 2.4. Oil Red O staining

Oil Red O powder was purchased from Sigma-Aldrich (St. Louis, MO). phosphate buffered saline (PBS) was purchased from Biosesang (Seoungnam, South Korea). Isopropyl alcohol was obtained from Amresco LLC (Solon, OH). 3T3-L1 preadipocytes were seeded in 24-well plate at a density of 5.0 x $10^4$ cells per well. After confluence, the cells were differentiated for 6 days with or without chemicals. Differentiated cells were subjected to Oil Red O staining to visualize accumulated lipid droplets in the cells. Media were removed and differentiated cells were fixed with 4% formalin for 20 min. followed by PBS washing. The fixed cells were then stained with Oil Red O solution for 15 min. at room temperature. Oil Red O solution was prepared by dissolving 0.25 mg Oil Red O powder in 50 mL 60% isopropyl alcohol followed by filtering with 0.45 μm membrane purchased from Whatman™ (Piscataway, NJ). After staining, the cells were washed three times with PBS. Intracellular lipid content was

quantified by eluting Oil Red O stain with isopropyl alcohol and measured at 515 nm with spectrophotometry (Beckman-Coulter, CA).

**2.5. Western blot assay**

The antibody against β-actin was purchased from Sigma-Aldrich (St. Louis, MO). CK1ε and eIF4E were purchased from Santa Cruz Biotechnology (Dallas, TX). Phosphorylated 4E-BP1 and 4E-BP1 were purchased from Cell Signaling Biotechnology (Danvers, MA). Phosphorylated eIF4E was purchased from EPITOMICS (Burlingame, CA). 3T3-L1 preadipocytes were seeded in 6-cm dishes at a density of $5.0 \times 10^4$ cells. After confluence, the medium was changed to a series of DMEM containing proper cocktail until fully differentiation. While the differentiation process, cells were treated with or without chemicals at indicated concentrations. Cells were harvested by scraping in cell lysis buffer and the protein concentration of each sample was determined by using ad dye-binding protein assay kit purchased from

Bio-Rad Laboratories (Hercules, CA) according to the manufacturer's instructions. Cell lysates were loaded and separated on sodium dodecyl sulfate polyacrylamide gel electrophoresis (SEMS-PAGE) gels and transferred onto polyvinylidene fluoride membrane purchased from EMD Millipore (Billerica, MA). The membranes were blocked with 5% skim milk and attached with specific primary antibodies followed by HRP-conjugated secondary antibodies. The protein bands were detected by a chemiluminescence detection kit purchased from Amersham Pharmacia Biotech (Piscataway, NJ).

**2.6. Kinase assay**

In brief, kinases were incubated with substrate or required cofactors. The reaction was initiated by the addition of the compound in DMSO and $^{33}$P-ATP (specific activity 10 μCi/μl). After incubation for 120 min at room temperature, the reaction was spotted onto P81 ion exchange paper purchased from GE Healthcare (Little Chalfont, UK)

and washed extensively in 0.75% phosphoric acid. Kinase activity data was expressed as the percent remaining kinase activity in test samples compared to vehicle (DMSO) reactions.

**2.7. Pull-down assay**

Sepharose 4B freeze-dried powder was purchased from GE Healthcare (Little Chalfont, UK). Sepharose 4B beads (0.3 g) were activated in 1 mM HCl and suspended in orobol (2 mg) coupled solution (0.1 M $NaHCO_3$ and 0.5 M NaCl). Following overnight rotation at 4 °C, the mixture was transferred to 0.1 M Tris-HCl buffer (pH 8.0) and rotated at 4 °C overnight again. The mixture was then washed with 0.1 M acetate buffer (pH 4.0), 0.1 M Tris-HCl, 0.5 M NaCl buffer (pH 8.0) and suspended in PBS. After beads were ready for use, active protein (CK1ε) was incubated with either sepharose 4B alone or orobol-sepharose 4B beads in reaction buffer. After incubation at 4 °C, the beads were washed with washing buffer and the proteins

bound to the beads were analyzed by immunoblotting.

**2.8. Animal study**

Male C57BL/6J mice (5-week-old) were purchased from Japan SLC (Hamamatsu, Shizuoka, Japan). The normal diet (ND) was purchased from Zeigler (Gardners, PA) and high-fat diet (HFD) was purchased from Research Diets (New Brunswick, NJ). Polyethylene glycol 200 (PEG 200) was purchased from Sigma-Aldrich (St. Louis, MO). After 1 week acclimation, mice were housed in climate-controlled quarters (23±3 1C, 50±10% humidity) with a 12-h light–dark cycle. Mice ($N^{1/3}30$) were divided into three different dietary groups (n=10 each group): ND, HFD, and a HFD-supplemented with 10 $mgkg^{-1}$ body weight (BW) of orobol. Diets were provided in the form of pellets for 23 weeks. Animals were treated with orobol, which was dissolved in 1% DMSO and 99% PEG 200, or vehicle (1% DMSO and 99% PEG200). Body weight and food intake were monitored on a

weekly basis.

### 2.9. Statistical analysis

For *in vitro* study, data were expressed as means ± standard error of the mean (SEM) and each control group were compared by Student's t-test. To compare the difference between the MDI treated groups, one-way ANOVA followed by Duncan′s statistical range test. Means with superscripts of different letters were significantly different at $p < 0.05$. The data were statistically analyzed with IBM SPSS Statistics ver. 22.0 (Armonk, NY).

# Ⅲ. Results

## 3.1. Orobol inhibits MDI-induced adipogenesis in 3T3-L1 preadipocytes

To compare the anti-adipogenic effect of soy isoflavones, such as genistin, daidzin, coumestrol, genistein, daidzein, and their metabolites, such as orobol, 6-ODI, equol, 3'-ODI, and 8-ODI, cells were treated with MDI and each chemical simultaneously with 20 μM. MDI significantly increased the relative lipid contents by 5-fold in 3T3-L1 preadipocytes compared to undifferentiated control. ORO staining indicated that orobol had the best anti-adipogenic effect among other soy isoflavones (Fig. 1B). To identify the difference between orobol and its precursor, genistein, ORO staining was conducted in a dose-dependent manner. MDI-induced lipid accumulation was reduced in the cells treated with 10 or 20 μM of orobol, respectively but not genistein (Fig. 1C, 1D). To identify whether the decreased lipid accumulation by

orobol was not attributable to diminished cell viability, MTT assay was performed. Orobol did not cause a considerable decline in cell viability up to 40 μM (Fig. 1F). Taken together, orobol inhibited adipogenesis effectively.

# Figure 1

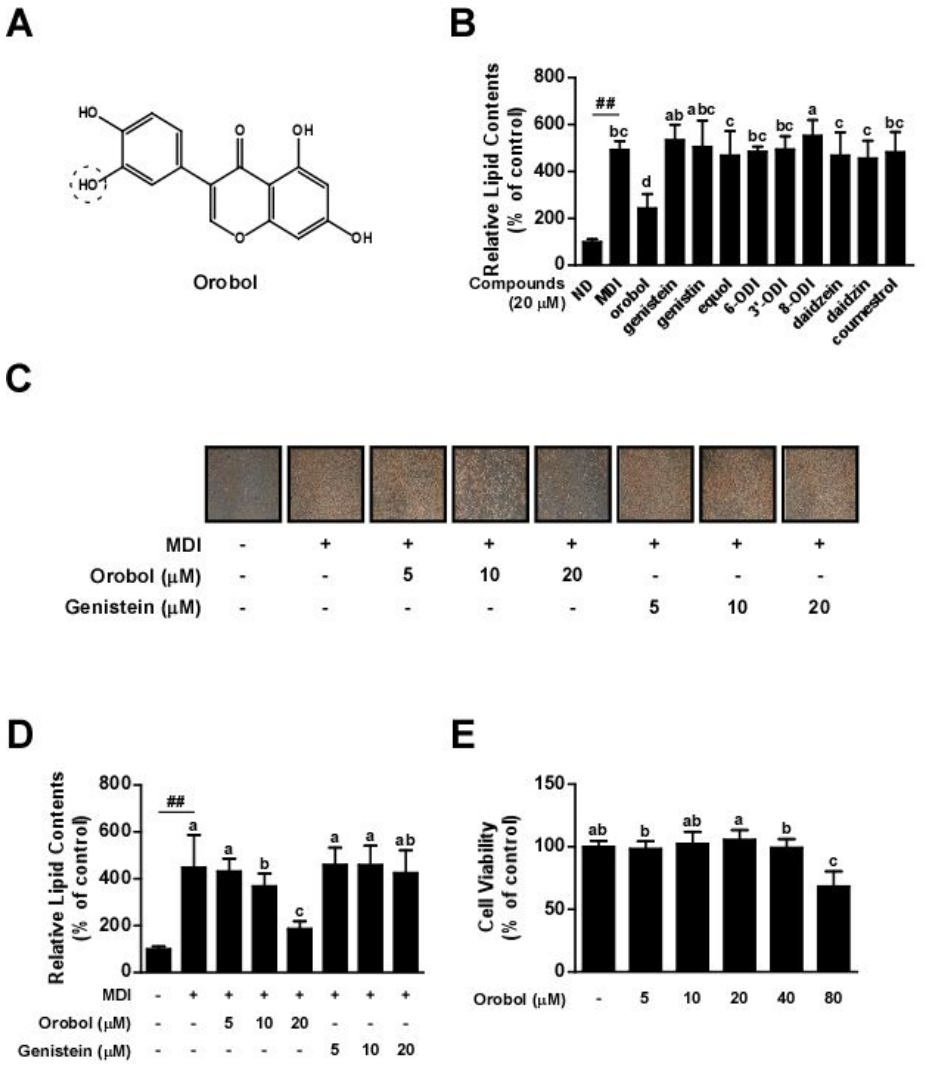
A
HO
HO
O
OH
O
OH
Orobol
B
Relative Lipid Contents (% of control)
800
600
400
200
0
##
bc
d
ab
abc
c
bc
bc
a
c
c
bc
Compounds (20 μM)
ND
MDI
orobol
genistein
genistin
equol
6-ODI
3'-ODI
8-ODI
daidzein
daidzin
coumestrol
C
MDI - + + + + + + +
Orobol (μM) - - 5 10 20 - - -
Genistein (μM) - - - - - 5 10 20
D
Relative Lipid Contents (% of control)
800
600
400
200
0
##
a
a
b
c
a
a
ab
MDI - + + + + + + +
Orobol (μM) - - 5 10 20 - - -
Genistein (μM) - - - - - 5 10 20
E
Cell Viability (% of control)
150
100
50
0
ab
b
ab
a
b
c
Orobol (μM) - 5 10 20 40 80

**Figure 1. Effects of orobol on MDI-induced adipogenesis and protein expression levels of FAS, PPARγ, and C/EBPα in 3T3-L1 preadipocytes**

(A) The chemical structure of orobol. (B) Orobol significantly inhibited the differentiation of 3T3-L1 preadipocytes among other soy isoflavones and their metabolites at 20 μM. (C) After cell differentiation, 3T3-L1 adipocytes were stained with Oil red O solution and images were captured. (D) Orobol inhibited MDI-induced adipogenesis in 3T3-L1 cells not genistein at the same concentration. (E) Orobol did not show cytotoxicity in 3T3-L1 preadipocytes up to 40 μM. Data are represented as mean ± SEM values of at least three independent experiments. The sharps (##) indicate a significant difference between the control group and the group treated with MDI cocktail alone ($p < 0.01$). Means with letters (a–d) within a graph are significantly different between groups treated with MDI alone and

those treated with MDI plus orobol or other soy isoflavones.

### 3.2. Orobol blocks MDI-induced lipid accumulation through all stages of adipogenesis in 3T3-L1 preadipocytes

Adipogenesis consists early, intermediate, and terminal phase of differentiation. To identify the key stage when orobol exerts its anti-adipogenic activity, orobol was treated at different stages of cellular differentiation (Fig. 2A). The most effective time of adipogenesis inhibition was the periods containing 0-2 days treated orobol. However, orobol significantly reduced lipid accumulation treated at any time periods (Fig. 2B). These results showed that orobol majorly diminished MDI-triggered lipid accumulation through all stages of adipogenesis.

**Figure 2**

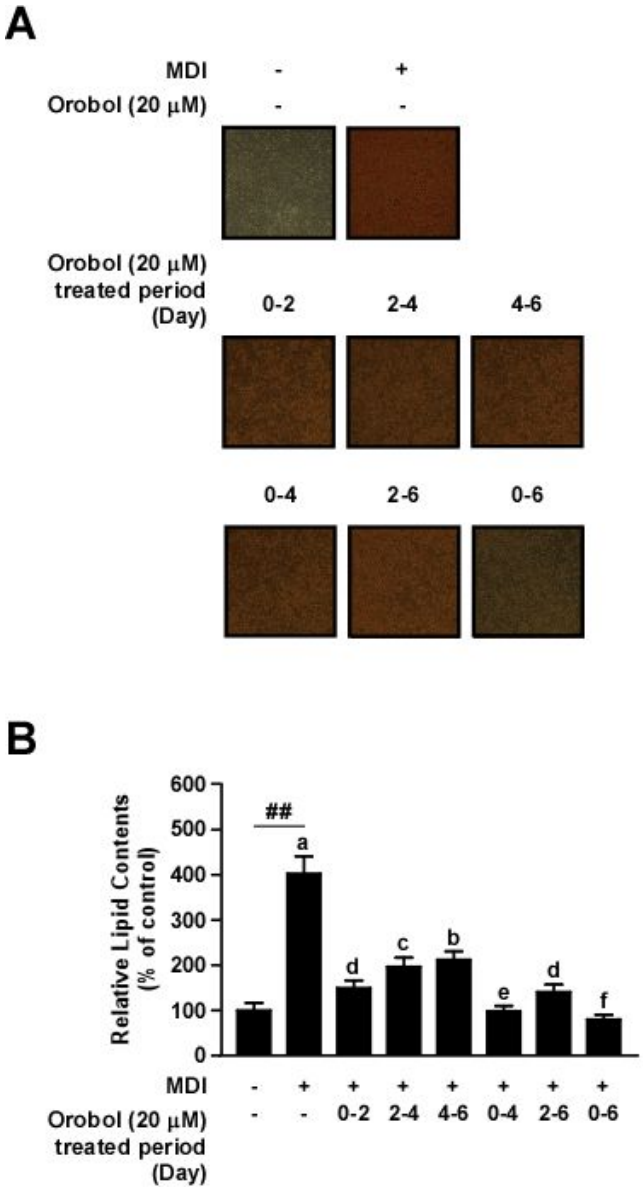
A
MDI
Orobol (20 μM)
Orobol (20 μM) treated period (Day)
0-2
2-4
4-6
0-4
2-6
0-6
B
Relative Lipid Contents (% of control)
600
500
400
300
200
100
0
##
a
b
c
d
e
d
f
MDI
Orobol (20 μM) treated period (Day)

**Figure 2. Effects of orobol on 3T3-L1 preadipocytes at different stages of MDI-induced adipogenesis**

(A-B) Confluent 3T3-L1 preadipocytes were differentiated into mature adipocytes in the presence of 20 μM orobol for the indicated time periods. (A) After differentiation, the images of 3T3-L1 adipocytes stained with Oil red O solution were captured. (B) Stained dishes were quantified via spectrophotometry. Data are represented as mean ± SEM values of at least three independent experiments. The sharps (##) indicate a significant difference between the control group and the group treated with MDI alone ($p < 0.01$). Means with letters (a–f) within a graph are significantly different between groups treated with MDI alone and those treated with MDI plus orobol treated at each of the different stage.

### 3.3. Orobol inhibits CK1ε kinase activity

Based on the previous study, CK1ε which inhibits 4E-BP1 function was chosen as the target kinase of orobol. 4E-BP1 is a regulator of representative adipogenesis marker, PPARγ and C/EBPα [33, 34]. To elucidate the effect of orobol on CK1ε function, I examined the CK1ε kinase activity treated with orobol at 2 μM. Orobol significantly attenuated the activity of the CK1ε kinase with the half maximal inhibitory concentration ($IC_{50}$) ($IC_{50}$ = 1.24 μM) (Fig. 3A). To examine whether the orobol-mediated reductions in CK1ε kinase activity occurs through a direct interaction between orobol and CK1ε kinase, a pull-down assay was conducted. The CK1ε kinase bound to orobol–sepharose 4B beads, but not to control sepharose 4B beads (Fig. 3B) getting the same result of CK1ε in cell lysate (Fig. 3C). These results collectively suggested that orobol directly bound to CK1ε kinase and inhibited its activity.

# Figure 3

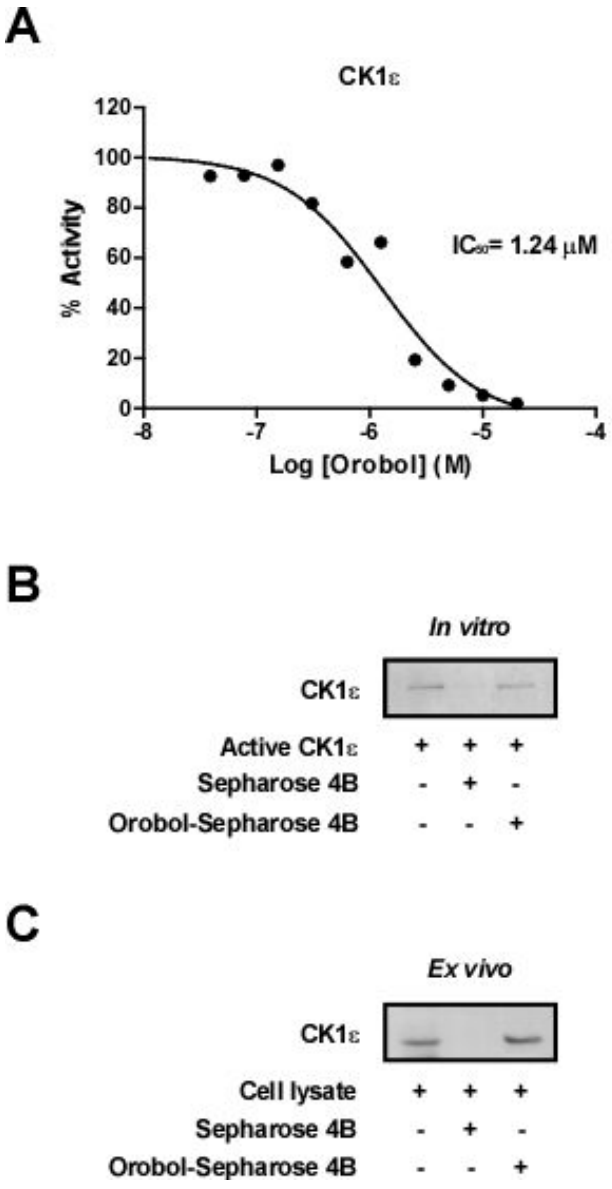
A
CK1ε
120
100
80
60
40
20
0
% Activity
IC50= 1.24 μM
-8
-7
-6
-5
-4
Log [Orobol] (M)
B
In vitro
CK1ε
Active CK1ε + + +
Sepharose 4B - + -
Orobol-Sepharose 4B - - +
C
Ex vivo
CK1ε
Cell lysate + + +
Sepharose 4B - + -
Orobol-Sepharose 4B - - +

**Figure 3. Inhibitory effects of orobol on CK1 epsilon kinase activity**

(A) Orobol was tested for CK1ε kinase inhibitory activity from ten concentrations with 2-fold serial dilutions starting at 20 μM. (B) Orobol bound to CK1ε kinase directly *in vitro*. The binding orobol was evaluated by immunoblotting using an antibody against CK1ε; lane 1, CK1ε kinase; lane 2, CK1ε kinase precipitated with sepharose 4B, and lane 3, CK1ε kinase bound to orobol-sepharose 4B beads. (C) Orobol directly interacted with CK1ε in 3T3-L1 cell lysate. The CK1ε kinase bound to orobol was evaluated by immunoblotting; lane 1, CK1ε kinase in whole lysate of 3T3-L1 cells; lane 2, CK1ε kinase in lysate precipitated with sepharose 4B beads; lane 3, CK1ε kinase in whole lysate of 3T3-L1 cells precipitated by orobol-sepharose 4B beads. The data are representative of three independent experiments that give similar results.

### 3.4. Orobol suppresses 4E-BP1 phosphorylation in 3T3-L1 preadipocytes

To examine whether orobol downregulates phosphorylation of 4E-BP1 known as the downstream marker of CK1ε, western blot assay was conducted. Orobol effectively suppressed MDI induced phosphorylation of 4E-BP1 but not its downstream signal (Fig. 4A). 4E-BP1 regulates negatively the eIF4E by binding not phosphorylation [35]. PPARγ, C/EBPα, and FAS are master regulators of adipogenesis [32]. The protein expression levels of these proteins were attenuated by 10 or 20 μM of orobol in 3T3-L1 preadipocytes treated with MDI (Fig. 1D). Collectively, these findings indicated that orobol inhibited 4E-BP1-mediated adipogenesis signaling pathways stimulated by MDI.

**Figure 4**

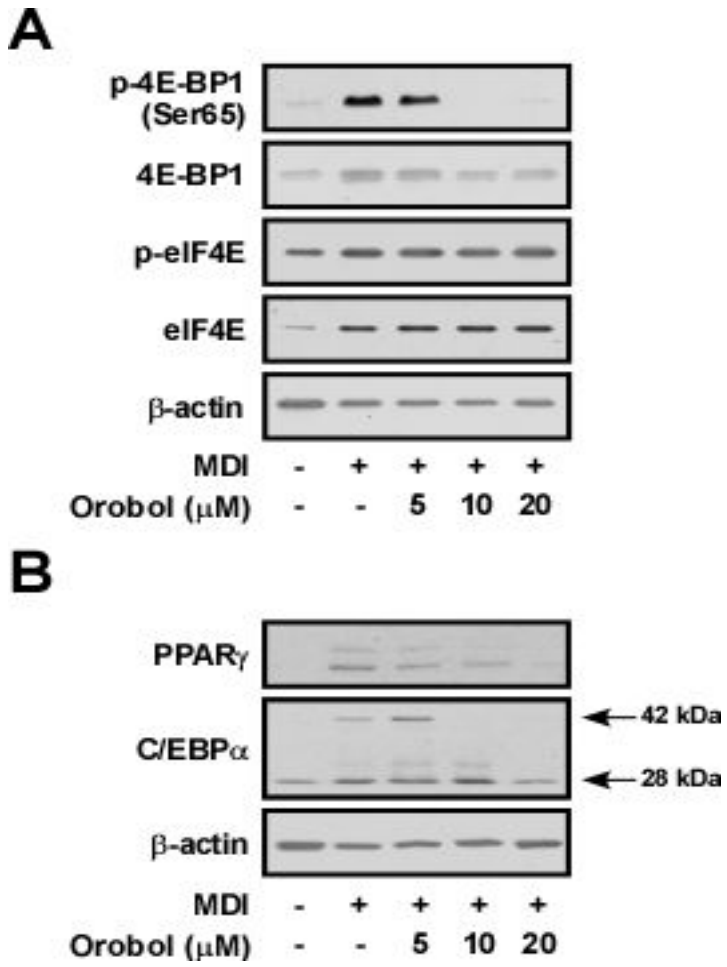
A
p-4E-BP1 (Ser65)
4E-BP1
p-eIF4E
eIF4E
β-actin
MDI - + + + +
Orobol (μM) - - 5 10 20
B
PPARγ
C/EBPα
42 kDa
28 kDa
β-actin
MDI - + + + +
Orobol (μM) - - 5 10 20

**Figure 4. Effects of orobol on MDI-induced 4E-BP1 signaling pathway of 3T3-L1 preadipocytes**

(A) The protein expression levels of phospho- and total-4E-BP1 was downregulated by orobol dose dependently but not phospho- and total-eIF4E proteins. (B) Orobol suppressed the expression of FAS, PPARγ, and C/EBPα in 3T3-L1 preadipocytes. Arrows marked on the band of C/EBPα point to specific C/EBPα proteins. The data are representative of three independent experiments that give similar results.

### 3.5. Orobol ameliorates obesity in HFD-fed mice

To further investigate anti-obesity effects of orobol, mice were fed HFD with or without orobol 10 $mgkg^{-1}$ BW for 23 weeks. Photographic data showed that orobol caused less obese phenotype, which might be associated with decreased fat accumulation (Fig. 5A). The average body weight of HFD-fed mice (43.72±1.41 g) was about 30.5% higher than that of control mice (30.40±0.72 g). Administration of orobol 10 $mgkg^{-1}$ BW significantly reduced body weight by 17.3% compared to HFD group ($p < 0.05$; Fig. 5B). The autopsy results indicated that orobol significantly reduced visceral fat mass such as epididymal, retroperitoneal, and perirenal fat in HFD-fed mice ($p < 0.05$; Fig. 5C, 5D, 5E). Also orobol showed a decreasing tendency in subcutaneous fat mass in HFD-fed mice ($p = 0.071$; Fig. 5F). There were no significant differences ($p > 0.05$) in daily calorie intake (Kcal per day) between HFD and orobol 10 mg $kg^{-1}$ BW groups (Fig. 5G). Taken together, orobol attenuated HFD-induced body weight gain and

lipid accumulation not affecting food intake.

# Figure 5

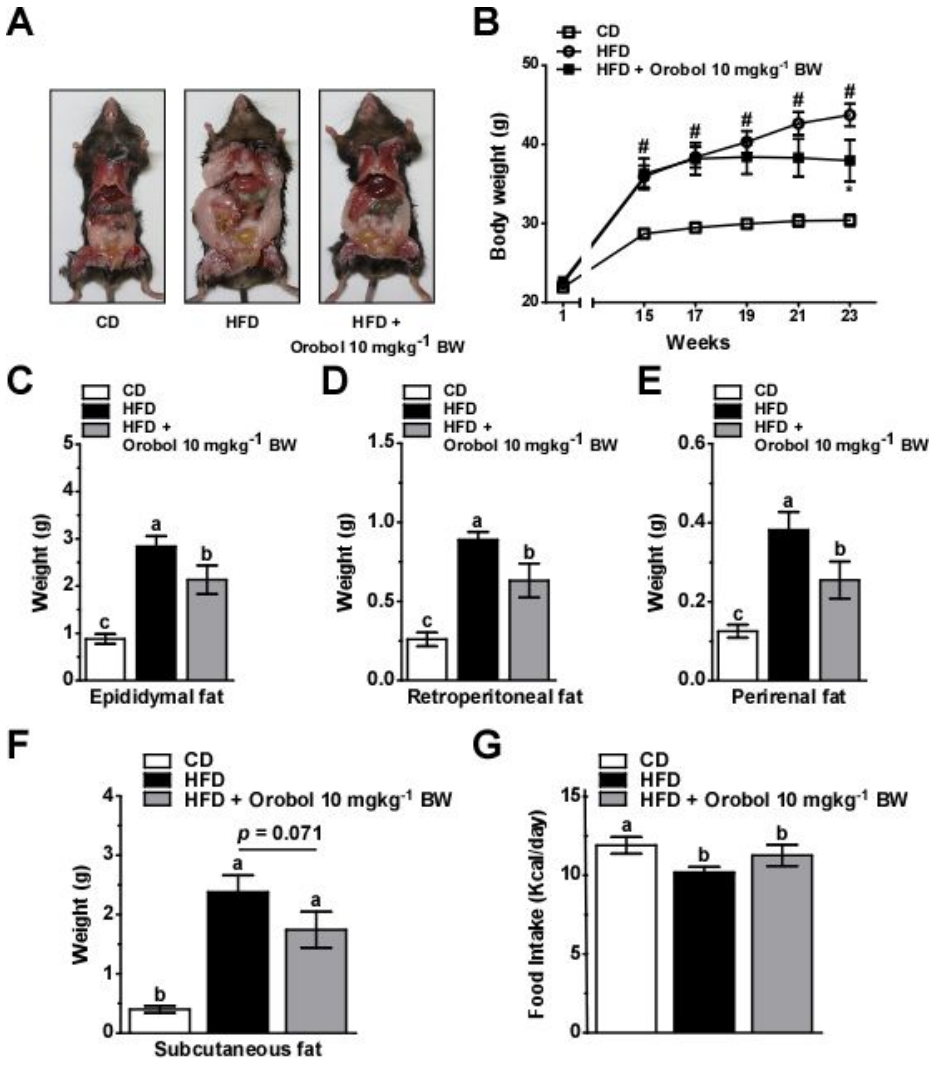
A
CD
HFD
HFD + Orobol 10 mgkg-1 BW
B
CD
HFD
HFD + Orobol 10 mgkg-1 BW
Body weight (g)
Weeks
C
Weight (g)
Epididymal fat
D
Retroperitoneal fat
E
Perirenal fat
F
p = 0.071
Subcutaneous fat
G
Food Intake (Kcal/day)

**Figure 5. Effects of orobol on HFD-induced obesity in C57BL/6J mice**

(A) The photographs at autopsy of C57BL/6J mice showed reduced fat mass by orobol. (B) Orobol treatment for 23 weeks alleviated HFD-induced weight gain in C57BL/6J mice. (C-E) The estimated weight of adipose tissue indicated that orobol decreased epididymal fat, retroperitoneal fat, and perirenal fat masses. (F) But orobol has no significant effect on subcutaneous fat mass. (G) The calorie intakes were unaffected by orobol (10 mgkg-1 BW). Values were expressed as means ± SEM values. The means marked with superscript letters were significantly different ($p < 0.05$).

## Ⅳ. Discussion

Orobol is one of the isoflavones derived from soybean. Orobol can be found in nature or fermented food, also can be generated by the bioconversion from genistein which has anti-obesity effects [24, 29, 30, 38, 39]. Recently, it has been reported that a metabolite of soy isoflavone, 6,7,4'-trihydroxyisoflavone exerts more anti-adipogenic effect than its precursor, daidzein [40]. Although considerable anti-obesity effects are expected, there has been a limitation to research orobol due to production technology. This issue has been resolved using tyrosinase which leads to o-hydroxylation. [41, 42].

CK1ε has essential functions in diverse cellular processes including transcription and translation that generate circadian rhythm in mammals [19-20]. CK1ε serves as the key regulator of circadian period [49]. Previous studies discovered that disruption of the circadian clock has been linked to obesity and metabolic diseases [16, 50, 51]. 4E-BP1

is a substrate of CK1ε. 4E-BP1/eIF4E is one of the major signal transduction pathways modulating cell proliferation and differentiation [13-15]. Also, 4E-BP1 is an important factor for control of PPARγ and C/EBPα which are master regulators of adipogenesis [34]. Previous studies have shown that mTORC1 affects adipogenesis via 4E-BP1/eIF4E pathway [11, 12, 43-45]. However, several studies have reported that mTORC1 inhibitors do not considerably inhibit 4E-BP1 phosphorylation and cell proliferation in many cell types [46-48]. Interestingly, a recent study revealed that CK1ε is a major regulator of 4E-BP1 [21]. Differentiation to adipocytes causes increase of adipose tissue, and induces obesity. The molecular mechanism of adipocyte differentiation have been widely examined in the murine preadipicyte cell line, 3T3-L1. My data show that orobol plays a key role in regulating CK1ε activity by direct binding, therefore it modulates adipogenic gene expression through entire differentiation time periods in 3T3-L1. And unchanged phosphorylation of eIF4E seems to be

because 4E-BP1 regulates it by binding. Furthermore, it is required to determine whether orobol binds to CK1ε in an ATP competitive manner and how orobol regulates the downstream signaling pathways. This is the first discovery that regulates adipogenesis through CK1ε/4E-BP1 pathway.

*In vitro* study was further supported by the *in vivo* evidence. High-fat, high-calorie diets are associated with obesity. In this study, HFD-fed mouse used as an obesity model. The animal study indicated that orobol 10 $mgkg^{-1}$ BW has an effect on obesity. Lower body weight gain was likely due to decreased fat mass especially visceral fat. A greater accumulation of visceral adipose tissue is an important risk factor for metabolic diseases [36, 37]. Therefore, orobol can be expected beneficial effects on metabolic disorders as well. Further animal studies are required to determine the mechanism of CK1ε and

adipogenesis. Also it is necessary that which physiological levels of orobol regulates obesity in humans.

In summary, this study provides the first evidence that orobol inhibits adipogenesis in 3T3-L1 by reducing CK1ε kinase activity via direct binding. Orobol also exhibits anti-obesity activity in diet-induced obese mice, which is attributable to decreased adipose tissue mass. This suggests a potential of orobol to prevent obesity by targeting CK1ε in tissue-specific manner. Orobol is expected as a new natural compound for obesity treatment.

## Ⅴ. References


1. van der Klaauw, A.A. and I.S. Farooqi, *The Hunger Genes: Pathways to Obesity.* Cell, 2015. **161**(1): p. 119-132.
2. Rosen, E.D., *Two paths to fat.* Nature cell biology, 2015. **17**(4): p. 360-361.
3. Wang, Q.A., et al., *Tracking adipogenesis during white adipose tissue development, expansion and regeneration.* Nature medicine, 2013. **19**(10): p. 1338-1344.
4. Stephens, J.M., *The fat controller: adipocyte development.* 2012.
5. Rodríguez, A., et al., *Revisiting the adipocyte: a model for integration of cytokine signaling in the regulation of energy metabolism.* American Journal of Physiology-Endocrinology and Metabolism, 2015. **309**(8): p. E691-E714.
6. Moreno-Navarrete, J.M. and J.M. Fernández-Real, *Adipocyte differentiation*, in *Adipose tissue biology*. 2012, Springer. p. 17-38.
7. Fajas, L., *Adipogenesis: a cross-talk between cell proliferation and cell differentiation.* Annals of medicine, 2003. **35**(2): p. 79-85.

8. Tsukiyama-Kohara, K., et al., *Adipose tissue reduction in mice lacking the translational inhibitor 4E-BP1.* Nature medicine, 2001. **7**(10): p. 1128-1132.

9. Le Bacquer, O., et al., *Elevated sensitivity to diet-induced obesity and insulin resistance in mice lacking 4E-BP1 and 4E-BP2.* Journal of Clinical Investigation, 2007. **117**(2): p. 387.

10. Figarola, J.L. and S. Rahbar, *Small‐molecule COH-SR4 inhibits adipocyte differentiation via AMPK activation.* International journal of molecular medicine, 2013. **31**(5): p. 1166-1176.

11. Laplante, M. and D.M. Sabatini, *An emerging role of mTOR in lipid biosynthesis.* Current Biology, 2009. **19**(22): p. R1046-R1052.

12. El-Chaar, D., A. Gagnon, and A. Sorisky, *Inhibition of insulin signaling and adipogenesis by rapamycin: effect on phosphorylation of p70 S6 kinase vs eIF4E-BP1.* International journal of obesity, 2004. **28**(2): p. 191-198.

13. Azar, R., et al., *4E-BP1 is a target of Smad4 essential for TGFβ-mediated inhibition of cell proliferation.* The EMBO journal, 2009. **28**(22): p. 3514-3522.

14. Richter, J.D. and N. Sonenberg, *Regulation of cap-dependent*

*translation by eIF4E inhibitory proteins.* Nature, 2005. **433**(7025): p. 477-480.

15. Pons, B., et al., *The effect of p-4E-BP1 and p-eIF4E on cell proliferation in a breast cancer model.* International journal of oncology, 2011. **39**(5): p. 1337-1345.

16. Turek, F.W., et al., *Obesity and metabolic syndrome in circadian Clock mutant mice.* Science, 2005. **308**(5724): p. 1043-1045.

17. Bray, M. and M. Young, *Circadian rhythms in the development of obesity: potential role for the circadian clock within the adipocyte.* obesity reviews, 2007. **8**(2): p. 169-181.

18. Sahar, S. and P. Sassone-Corsi, *Metabolism and cancer: the circadian clock connection.* Nature Reviews Cancer, 2009. **9**(12): p. 886-896.

19. Knippschild, U., et al., *The casein kinase 1 family: participation in multiple cellular processes in eukaryotes.* Cellular signalling, 2005. **17**(6): p. 675-689.

20. Kim, S.Y., et al., *CK1epsilon is required for breast cancers dependent on beta-catenin activity.* PLoS One, 2010. **5**(2): p. e8979.

21. Shin, S., et al., *Casein Kinase 1ε promotes cell proliferation by*

*regulating mRNA translation.* Cancer research, 2014. **74**(1): p. 201-211.

22. Yun, J.W., *Possible anti-obesity therapeutics from nature–A review.* Phytochemistry, 2010. **71**(14): p. 1625-1641.

23. Orgaard, A. and L. Jensen, *The effects of soy isoflavones on obesity.* Experimental Biology and Medicine, 2008. **233**(9): p. 1066-1080.

24. Klus, K. and W. Barz, *Formation of polyhydroxylated isoflavones from the soybean seed isoflavones daidzein and glycitein by bacteria isolated from tempe.* Archives of microbiology, 1995. **164**(6): p. 428-434.

25. Kiriakidis, S., et al., *Novel tempeh (fermented soyabean) isoflavones inhibit in vivo angiogenesis in the chicken chorioallantoic membrane assay.* British journal of nutrition, 2005. **93**(03): p. 317-323.

26. Behloul, N. and G. Wu, *Genistein: a promising therapeutic agent for obesity and diabetes treatment.* European journal of pharmacology, 2013. **698**(1): p. 31-38.

27. Yang, J.-Y., et al., *Effect of genistein with carnitine administration on lipid parameters and obesity in C57Bl/6J*

*mice fed a high-fat diet.* Journal of Medicinal Food, 2006. **9**(4): p. 459-467.

28. Kim, H.-K., et al., *Genistein decreases food intake, body weight, and fat pad weight and causes adipose tissue apoptosis in ovariectomized female mice.* The Journal of nutrition, 2006. **136**(2): p. 409-414.

29. Preedy, V.R., *Isoflavones: chemistry, analysis, function and effects*. 2012: Royal Society of Chemistry.

30. Nguyen, D.T., et al., *The intracellular genistein metabolite 5, 7, 3', 4'-tetrahydroxyisoflavone mediates G2-M cell cycle arrest in cancer cells via modulation of the p38 signaling pathway.* Free Radical Biology and Medicine, 2006. **41**(8): p. 1225-1239.

31. Vauzour, D., et al., *Inhibition of cellular proliferation by the genistein metabolite 5, 7, 3', 4'-tetrahydroxyisoflavone is mediated by DNA damage and activation of the ATR signalling pathway.* Archives of biochemistry and biophysics, 2007. **468**(2): p. 159-166.

32. Cristancho, A.G. and M.A. Lazar, *Forming functional fat: a growing understanding of adipocyte differentiation.* Nature reviews Molecular cell biology, 2011. **12**(11): p. 722-734.

33. Ruggero, D., *Translational control in cancer etiology.* Cold Spring Harbor perspectives in biology, 2013. **5**(2): p. a012336.

34. Blagden, S.P. and A.E. Willis, *The biological and therapeutic relevance of mRNA translation in cancer.* Nature reviews Clinical oncology, 2011. **8**(5): p. 280-291.

35. Gingras, A.-C., et al., *Regulation of 4E-BP1 phosphorylation: a novel two-step mechanism.* Genes & development, 1999. **13**(11): p. 1422-1437.

36. Bergman, R.N., et al., *Why visceral fat is bad: mechanisms of the metabolic syndrome.* Obesity, 2006. **14**(S2): p. 16S-19S.

37. Matsuzawa, Y., et al., *Pathophysiology and pathogenesis of visceral fat obesity.* Obesity research, 1995. **3**(S2): p. 187s-194s.

38. Kiriakidis, S., et al., *Novel tempeh (fermented soyabean) isoflavones inhibit in vivo angiogenesis in the chicken chorioallantoic membrane assay.* Br J Nutr, 2005. **93**(3): p. 317-23.

39. Park, H.Y., et al., *A new isoflavone glycoside from the stem bark of Sophora japonica.* Archives of pharmacal research, 2010. **33**(8): p. 1165-1168.

40. Seo, S.G., et al., *A metabolite of daidzein, 6, 7, 4'-*

*trihydroxyisoflavone, suppresses adipogenesis in 3T3-L1 preadipocytes via ATP-competitive inhibition of PI3K.* Molecular nutrition & food research, 2013. **57**(8): p. 1446-1455.

41. Lee, S.H., et al., *Using tyrosinase as a monophenol monooxygenase: A combined strategy for effective inhibition of melanin formation.* Biotechnology and bioengineering, 2015.

42. Choi, K.Y., et al., *Development of Colorimetric HTS Assay of Cytochrome P450 for ortho-Specific Hydroxylation, and Engineering of CYP102D1 with Enhanced Catalytic Activity and Regioselectivity.* Chembiochem, 2013. **14**(10): p. 1231-1238.

43. Rosen, E.D. and O.A. MacDougald, *Adipocyte differentiation from the inside out.* Nature reviews Molecular cell biology, 2006. **7**(12): p. 885-896.

44. Kim, J.E. and J. Chen, *Regulation of peroxisome proliferator–activated receptor-γ activity by mammalian target of rapamycin and amino acids in adipogenesis.* Diabetes, 2004. **53**(11): p. 2748-2756.

45. Polak, P., et al., *Adipose-specific knockout of raptor results in lean mice with enhanced mitochondrial respiration.* Cell

metabolism, 2008. **8**(5): p. 399-410.

46. Ducker, G.S., et al., *Incomplete inhibition of phosphorylation of 4E-BP1 as a mechanism of primary resistance to ATP-competitive mTOR inhibitors.* Oncogene, 2014. **33**(12): p. 1590-1600.

47. Choo, A.Y., et al., *Rapamycin differentially inhibits S6Ks and 4E-BP1 to mediate cell-type-specific repression of mRNA translation.* Proceedings of the National Academy of Sciences, 2008. **105**(45): p. 17414-17419.

48. Zhang, Y. and X.S. Zheng, *mTOR-independent 4E-BP1 phosphorylation is associated with cancer resistance to mTOR kinase inhibitors.* Cell Cycle, 2012. **11**(3): p. 594-603.

49. Meng, Q.-J., et al., *Setting clock speed in mammals: the CK1ε tau mutation in mice accelerates circadian pacemakers by selectively destabilizing PERIOD proteins.* Neuron, 2008. **58**(1): p. 78-88.

50. Leone, V., et al., *Effects of Diurnal Variation of Gut Microbes and High-Fat Feeding on Host Circadian Clock Function and Metabolism.* Cell host & microbe, 2015. **17**(5): p. 681-689.

51. Summa, K.C. and F.W. Turek, *Chronobiology and obesity:*

*interactions between circadian rhythms and energy regulation.* Advances in Nutrition: An International Review Journal, 2014. **5**(3): p. 312S-319S.

# Ⅵ. 국문 초록

전 세계적으로 과체중 및 비만인구의 증가는 국가의 주요한 문제로 대두되고 있다. 오로볼(orobol)은 콩 이소플라본 중 하나로, 생산기술의 한계로 인해 많은 연구가 진행되지 않았다. 본 연구에서는 오로볼을 이용하여 3T3-L1 지방전구세포의 분화 억제 효능 및 동물에서의 비만 억제효능을 확인하고, 관련 메커니즘 규명 및 분자표적 발굴에 관한 연구를 수행하였다. 오로볼은 지방세포분화의 주요 조절 마커인 PPARɣ, C/EBPα, FAS 발현을 감소시킴으로써 3T3-L1 지방전구세포의 지방축적과정을 농도 의존적으로 저해 하였다. 오로볼의 지방세포분화 억제 효능은 전체 분화과정을 억제함으로써 나타났다. 이는 CK1ε 인산화 효소의 활성을 저해하여 그 하위 기질인 4E-BP1의 인산화를 억제하여 이루어짐을 관찰하였다. 또한 오로볼은 C57BL/6J 동물모델에서 지방조직의 무게를 감소시킴으로써 고지방 식이로 유도한 비만을 효과적으로 억제하였다. 종합적으로 연구의 결과들을 통해 오로볼이 CK1ε의 활성을 억제함으로써 3T3-L1의 지방세포분화형성을 저해하고, 고지방 식이로 유도한 동물모델에서 역시 비만을 억제하는 것을 확인

할 수 있었다. 본 연구에서는 오로볼의 항 비만효능 및 메커니즘을 최초로 규명하였으며, 세포 내 활성구조의 천연물질인 오로볼을 기존 부작용이 높은 합성 비만치료약과 낮은 효능을 지닌 항 비만 천연소재들의 한계점을 극복한 대안책으로 제시하였다.

주요어 : 오로볼; 비만; 지방세포분화형성; CK1ε; 3T3-L1 지방전구세포; C57BL/6J

학번 : 2014-20720